Supporting Information

Elucidation of Isomerization Pathways of a Single Azobenzene Derivative using an STM

*Emiko Kazuma, Mina Han, Jaehoon Jung, Junepyo Oh, Takahiro Seki, and Yousoo Kim**

Synthesis

4-Isopropoxy-3'-methoxyazobenzene (IMA): IMA was synthesized by reacting the precursor (4-[3'-methoxyphenylazo]phenol, 1.30 g, 4.81 mmol) with 2-bromopropane (0.89 g, 7.21 mmol) in N,N-dimethylformamide (50 mL) in the presence of K_2CO_3 (1.33 g, 9.62 mmol). The reaction mixture was stirred at 90 °C for 3 h and then cooled to room temperature, following which water and ethyl acetate were added. The organic layer was then separated and the solvent was removed by rotary evaporation. The residue was purified by silica gel column chromatography (hexane/dichloromethane = 10:1 (v/v)) and characterized by ^{1}H and ^{13}C NMR spectroscopy and fast atom bombardment (FAB) mass spectroscopy. (0.29 g, yield: 22%).

^{1}H NMR (300 MHz, $CDCl_3$) δ 7.88 (d, 2H, aromatic), 7.39-7.49 (m, 3H, aromatic), 6.98 (m, 3H, aromatic), 4.62 (sep, 1H, ArOC*H*$(CH_3)_2$), 3.87 (s, 3H, ArOC*H*$_3$), 1.37 (d, 6H, ArOCH(C*H*$_3)_2$). ^{13}C NMR (300 MHz, $CDCl_3$) δ 160.54, 160.24, 154.00, 146.56, 129.64, 124.77, 116.98, 116.61, 115.69, 105.53, 70.12, 55.37, 21.94. FAB-MS (m/z); found, 270.1381, calcd for $C_{16}H_{18}N_2O_2$ = 270.1368.

Details of the STM experiments

Ag(111) was cleaned using repeated cycles of Ar^+ ion sputtering and annealing at ~850 K. The IMA powder was degassed by freeze-pump-thaw cycles. The IMA molecules were deposited by evaporation from a glass ampule heated at 333 K. The Ag(111) substrate was maintained at <50 K during deposition. The sample was transferred to a low-temperature STM (Omicron GmbH) maintained under ultra-high vacuum below 5×10^{-11} Torr. All the STM measurements were performed at 5 K.

Figures

Both *cis*-A and *cis*-B have 6 equivalent adsorption orientations on the as-adsorbed Ag(111) surface, reflecting the six-fold symmetry of the Ag(111) substrate surface, as shown in Figure S1.

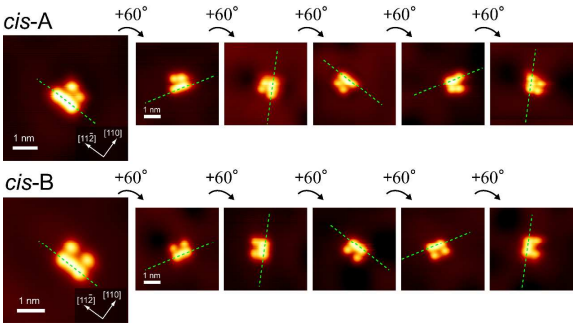

Figure S1 STM images of *cis*-A and *cis*-B on the as-adsorbed Ag(111) surface.

Reversible structural changes between *cis*-A and *cis*-B were achieved by injecting tunneling electrons from the STM tip with the feedback loop turned off, after placing the tip above the N=N bond of the molecule. The structural changes manifest as sudden changes in the corresponding current traces due to the change in the distance between the tip and sample (Figures S2a and S2b). Structural changes always accompany adsorption orientation changes, because the energy barriers for the orientation changes (Figure S3) are lower than those for the structural changes (Figure S2c). Reversible *cis-trans* isomerization was also achieved by the sequential injection of tunneling electrons into the molecule (Figures 2d-g).

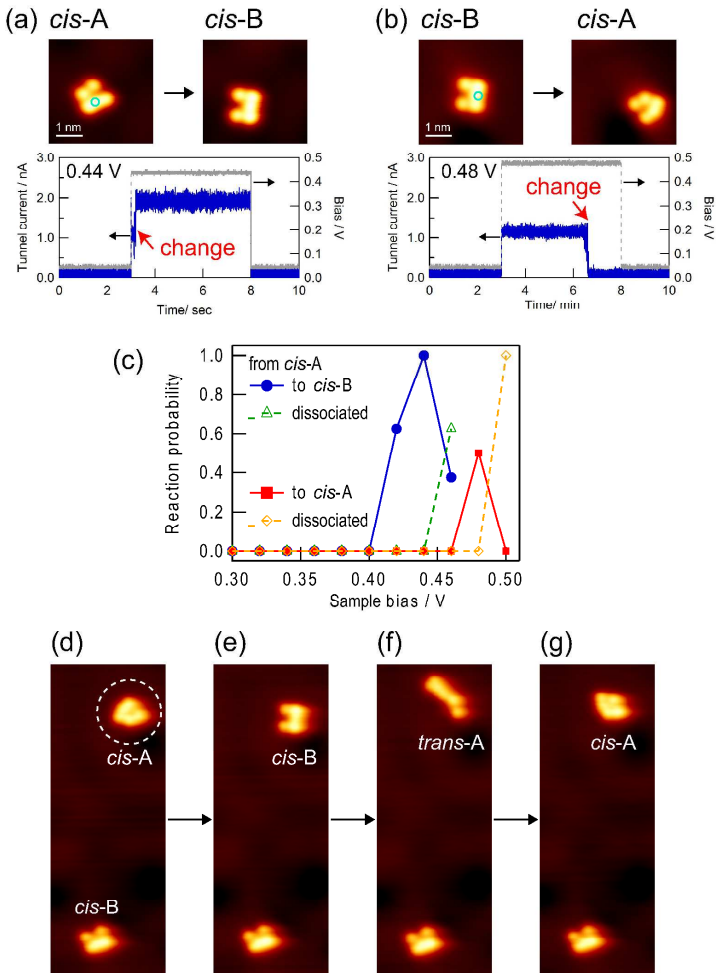

Figure S2 STM images and current traces corresponding to the structural changes (a) from *cis*-A to *cis*-B and (b) from *cis*-B to *cis*-A, induced by injecting tunneling electrons at the positions indicated by the blue circles. The sample bias, tunneling current, and time for the applied voltage pulse were (a) 0.44 V, 1.0 nA, 5 s and (b) 0.48 V, 1.0 nA, 5 s, respectively. (c) The reaction probabilities of the structural changes between *cis*-A and *cis*-B as a function of the sample bias voltage at 1.0 nA for 5 s. (d-g) STM images (d) before and (e-g) after the sequential injection of tunneling electrons into the molecule encircled by white dots in (d). The sample bias (V_s), tunneling current (I_t), and time (t) for the applied voltage pulse are [0.45 V, 1.0 nA, 5 s], [1.6 V, 1.0 pA, 5 s], and [0.5 V, 1.0 pA, 5 s] for (e), (f), and (g), respectively. The STM images were measured at 0.1 V and 0.1 nA.

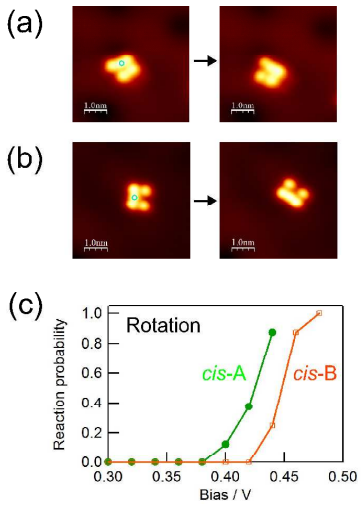

Figure S3 STM images before and after adsorption orientation changes induced by the injection of tunneling electrons for (a) *cis*-A and (b) *cis*-B. The sample bias, tunneling current, and time for the applied voltage pulse were (a) 0.40 V, 1.0 nA, 5 s and (b) 0.44 V, 1.0 nA, 5 s, respectively. (c) The probabilities of rotational motions for *cis*-A and *cis*-B as a function of the sample bias voltage.

The *trans* isomers exhibit a variety in the STM images (Figure S4), because the alkyl chains of the functional alkoxy groups attached to the phenyl rings may have rotational degree of freedom. In fact, the appearance of the two alkoxy groups at both phenyl rings in *trans*-A changed gradually during scanning even at a low sample bias voltage (Figure S4a). On the other hand, the azobenzene backbone remains rigidly fixed because the oxygen atoms of the two alkoxy groups at both phenyl rings strongly interact with the Ag(111) surface. Further, the structural changes between trans-A and trans-B, which is accompanied with the rotational motion of isopropoxy group, never happen.

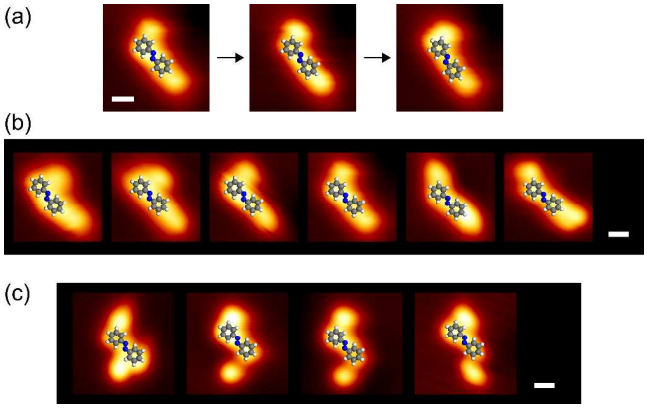

Figure S4 (a) Sequential changes in the STM images of typical *trans*-A during scanning at 0.05 V and 0.1 nA, due to the rotational motions of the functional alcoxy groups attached to the phenyl rings. (b, c) Variations in the STM images of (b) *trans*-A and (c) *trans*-B superimposed with schematic models of the azobenzene backbone. The scale bars represent 0.5 nm.

The photoswitching properties of the IMA molecules were observed in ethanol solution. The sample was irradiated alternatively with UV (350-375 nm, ~1 mW cm^{-2}) and blue (450 nm, ~1 mW cm^{-2}) light at room temperature. The extinction spectra were collected by a UV/Vis spectrophotometer (UV-3600, Shimadzu).

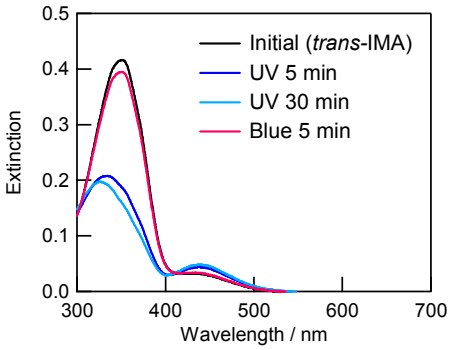

Figure S5 UV-visible extinction spectra of the IMA molecules in ethanol solution before and after alternate irradiation with UV (350-375 nm, ~1 mW cm^{-2}) and blue (450 nm, ~1 mW cm^{-2}) light.

Computational details

Density functional theory (DFT) calculations were performed for the isolated IMA molecules to determine the molecular structures observed in the STM images, because more realistic periodic system for single molecule adsorption requires not only a number of geometric adsorption configurations to find local minima but also huge size of supercell to separate molecules and thus high computational cost. To achieve sufficient geometric configurations, we considered a number of initial structures for *cis*-IMA and *trans*-IMA, respectively, based on the variation of their dihedral angles in the molecular frame. The geometric optimizations were, therefore, carried out for more than one hundred initial structures. All the calculations were performed using the Gaussian09 program suite.[1] The Becke three parameter hybrid functional (B3LYP),[2] where non-local correlation was provided by Lee-Yang-Parr expression,[3] and 6-31G(d,p) basis set were employed to optimize molecular structures. From the computational results, we obtained 31 and 27 local minimum structures for *cis*-IMA and *trans*-IMA, respectively. Figure S6 and S7 show the optimized structures and relative energies for energetically stable 10 geometric isomers for *cis*-IMA and *trans*-IMA, respectively. In terms of total energy, *trans*-A and *cis*-B was found to be the most stable configurations among the *trans* and *cis* isomers, respectively, in which *trans*-A is more stable than *cis*-B by 15.63 kcal/mol.

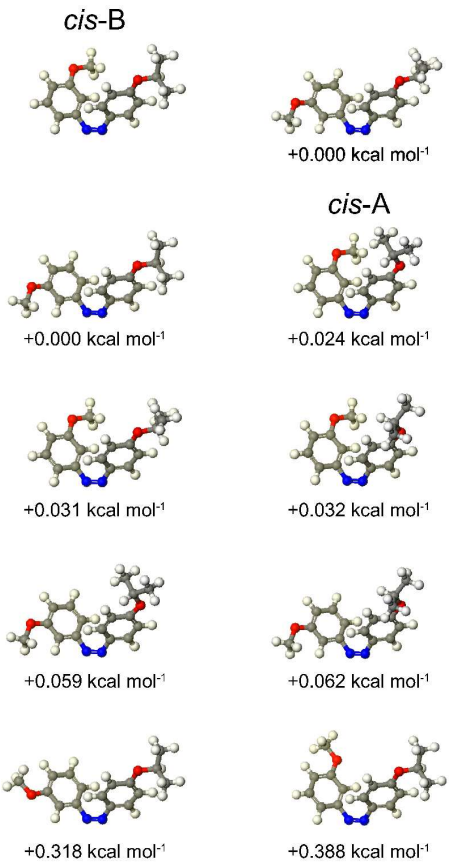

Figure S6 The most energetically stable 10 geometric isomers for *cis*-IMA in the gas phase obtained by DFT calculations. The energy differences against the most stable *cis*-isomer (*cis*-B) were also shown.

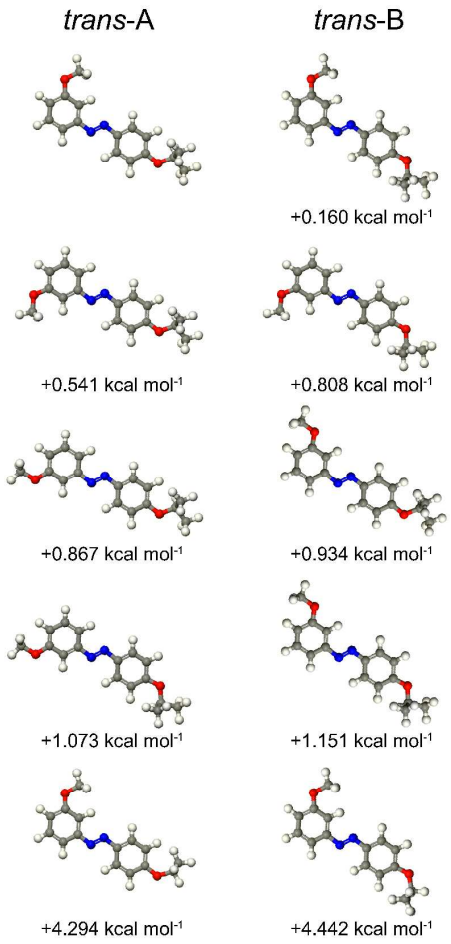

Figure S7 The most energetically stable 10 geometric isomers for *trans*-IMA in the gas phase obtained by DFT calculations. The energy differences against the most stable *trans*-isomer (*trans*-A) were also shown.

Cartesian coordinates (in Å) of *cis*-A

H	-6.038313	-1.447827	-1.418667
H	-6.013056	0.226032	-0.824444
H	-5.941299	-1.123742	0.324184
H	-3.836643	-2.850947	-1.29349
H	-3.830543	-2.545582	0.455082
H	-3.800773	-0.391653	-1.728933
H	-2.828263	1.689735	2.049075
H	-2.412415	-2.131135	-0.523471
H	-1.737244	-0.158612	-1.674075
H	-0.612361	2.854529	2.089958
H	0.454593	0.913434	-1.576946
H	0.818384	-1.915854	1.992776
H	1.726752	-3.303052	2.651527
H	1.812816	0.083335	1.452754
H	2.339877	-1.646484	2.8911
H	3.701979	1.546814	-2.102628
H	3.822654	-2.669093	-1.166091
H	4.388692	-0.784573	-2.694218
C	-5.616948	-0.779505	-0.662472
C	-4.102613	-0.777385	-0.745114
C	-3.505291	-2.157136	-0.514939
C	-2.425262	0.673106	0.207535
C	-2.090764	1.524006	1.270505
C	-1.500065	0.471921	-0.824901
C	-0.864021	2.160349	1.293671
C	-0.25199	1.080836	-0.771199
C	0.089513	1.915136	0.296952
C	1.82016	-2.316939	2.194539
C	2.375237	-0.12527	0.550744
C	2.684505	0.927617	-0.319677
C	2.795825	-1.415256	0.235638
C	3.436068	0.705278	-1.471482
C	3.511463	-1.653497	-0.945281
C	3.82191	-0.596253	-1.786916
N	1.280362	2.687992	0.381447
N	2.403756	2.281958	0.029885
O	-3.662965	0.134078	0.265094
O	2.554211	-2.503707	1.006351

Cartesian coordinates (in Å) of *cis*-B

H	-6.29792	0.483343	0.497143
H	-6.167549	-2.080606	0.012076
H	-5.680585	0.753886	-1.1451
H	-5.498815	-1.746937	-1.598215
H	-4.849814	1.473181	0.243879
H	-4.603879	-2.775947	-0.464317
H	-4.259533	-0.8534	1.047629
H	-3.069822	0.763359	1.634974
H	-1.305018	-0.143158	-2.176848
H	-1.055581	2.054862	2.238333
H	0.745534	1.08424	-1.525904
H	0.993672	-2.441932	1.284199
H	1.773456	-0.278046	1.401835
H	1.977091	-3.85023 6	1.766167
H	2.307958	-2.251235	2.481019
H	3.934984	2.188587	-1.353394
H	4.501021	-2.094279	-1.379805
H	5.013772	0.152134	-2.326857
C	-5.38925	0.588178	-0.103482
C	-5.24461	-1.894213	-0.544256
C	-4.537935	-0.667845	0.000544
C	-2.306163	0.193659	-0.314733
C	-2.240516	0.811336	0.93904
C	-1.221504	0.316619	-1.197311
C	-1.104619	1.533349	1.286957
C	-0.079243	0.999861	-0.826764
C	0.000711	1.604245	0.438209
C	1.999379	-2.777635	1.568508
C	2.485721	-0.203797	0.589148
C	2.769069	1.055168	0.043898
C	3.120999	-1.329338	0.069598
C	3.700559	1.196285	-0.982562
C	4.025012	-1.199336	-0.993167
C	4.303165	0.05637	-1.510952
N	1.057428	2.445109	0.88398
N	2.261976	2.249107	0.636087
O	-3.346473	-0.532774	-0.778585
O	2.924041	-2.591572	0.521919

Cartesian coordinates (in Å) of *trans*-A

H	-7.696076	0.818859	-0.771862
H	-7.336962	-0.761453	-0.046828
H	-6.804333	-0.405045	-1.700804
H	-6.47767	2.021365	1.203749
H	-6.20943	0.41604	1.912558
H	-5.253862	1.320858	-0.858646
H	-4.838193	1.501476	1.632208
H	-3.347987	1.824426	-0.189828
H	-3.149963	-2.465813	0.007929
H	-0.875979	1.921218 -	0.155841
H	-0.646912	-2.338065	0.048282
H	2.817314	1.270452	-0.096873
H	3.112147	-2.976339	0.18969
H	4.159265	2.993695	0.701407
H	4.188059	2.866959	-1.079682
H	5.539769	3.650676	-0.218145
H	5.619302	-2.814688	0.224872
H	6.704836	-0.576811	0.095183
C	-6.95006	0.021943	-0.705444
C	-5.797077	1.164907	1.229548
C	-5.643985	0.567082	-0.160544
C	-3.410342	-0.342374	-0.096478
C	-2.777354	0.904544	-0.14139
C	-2.631995	-1.512442	-0.025865
C	-1.38869	0.96456	-0.121365
C	-1.255911	-1.441983	-0.004526
C	-0.613166	-0.192735	-0.052739
C	2.850921	-0.860993	0.045542
C	3.459681	0.401152	-0.027711
C	3.620229	-2.0194	0.135677
C	4.806015	2.84462	-0.172809
C	4.845769	0.486939	-0.009267
C	5.010159	-1.918433	0.153952
C	5.624399	-0.678609	0.082606
N	0.777431	-0.002962	-0.036906
N	1.453679	-1.058451	0.033134
O	-4.744572	-0.544519	-0.129877
O	5.54299	1.648194	-0.075884

Cartesian coordinates (in Å) of *trans*-B

H	-7.709396	0.564481	-0.756534
H	-7.314584	-0.998387	-0.012475
H	-6.796491	-0.652834	-1.673365
H	-6.508921	1.81397	1.200422
H	-6.198678	0.224047	1.926728
H	-5.280026	1.116741	-0.860708
H	-4.855105	1.337979	1.624514
H	-3.387236	1.665021	-0.211965
H	-3.082607	-2.615707	0.051449
H	-0.924754	1.838908	-0.185259
H	-0.581191	-2.408751	0.0828
H	2.706369	3.000579	-0.188791
H	2.994707	-1.248676	0.065713
H	4.553462	-2.65694	1.066816
H	4.578665	-2.758581	-0.716009
H	5.211914	3.186926	-0.16054
H	6.018053	-3.23191	0.225946
H	6.592882	1.119352	-0.016855
C	-6.946748	-0.215885	-0.68301
C	-5.808273	0.974058	1.232158
C	-5.649743	0.363197	-0.15152
C	-3.396689	-0.502318	-0.084599
C	-2.789755	0.7626	-0.150157
C	-2.594117	-1.648169	0.001944
C	-1.408233	0.868957	-0.134635
C	-1.216984	-1.530923	0.017766
C	-0.604052	-0.273542	-0.050313
C	2.736795	0.868071	-0.062628
C	3.340371	2.122495	-0.126975
C	3.512298	-0.298523	0.018143
C	4.730918	2.214547	-0.110557
C	4.896883	-0.192088	0.033694
C	5.180456	-2.534856	0.174226
C	5.508767	1.070796	-0.03093
N	0.800013	-0.267836	-0.026724
N	1.325835	0.870553	-0.085138
O	5.746176	-1.246364	0.108654
O	-4.727348	-0.729354	-0.112967

References

[1] M. J. Frisch, G. W. Trucks, H. B. Schlegel, G. E. Scuseria, M. A. Robb, J. R. Cheeseman, G. Scalmani, V. Barone, B. Mennucci, G. A. Petersson, H. Nakatsuji, M. Caricato, X. Li, H. P. Hratchian, A. F. Izmaylov, J. Bloino, G. Zheng, J. L. Sonnenberg, M. Hada, M. Ehara, K. Toyota, R. Fukuda, J. Hasegawa, M. Ishida, T. Nakajima, Y. Honda, O. Kitao, H. Nakai, T. Vreven, J. A. Montgomery, Jr., J. E. Peralta, F. Ogliaro, M. Bearpark, J. J. Heyd, E. Brothers, K. N. Kudin, V. N. Staroverov, R. Kobayashi, J. Normand, K. Raghavachari, A. Rendell, J. C. Burant, S. S. Iyengar, J. Tomasi, M. Cossi, N. Rega, J. M. Millam, M. Klene, J. E. Knox, J. B. Cross, V. Bakken, C. Adamo, J. Jaramillo, R. Gomperts, R. E. Stratmann, O. Yazyev, A. J. Austin, R. Cammi, C. Pomelli, J. W. Ochterski, R. L. Martin, K. Morokuma, V. G. Zakrzewski, G. A. Voth, P. Salvador, J. J. Dannenberg, S. Dapprich, A. D. Daniels, Ö. Farkas, J. B. Foresman, J. V. Ortiz, J. Cioslowski, D. J. Fox, Gaussian 09, Revision B.1, Gaussian, Inc, Wallingford CT, 2009.

[2] A. D. Becke, *J. Chem. Phys.* **1993**, *98*, 5648-5652.

[3] C. Lee, W. Yang, and R. G. Parr, *Phys. Rev. B* **1998**, *37*, 785-789.